

Surface wettability of titania thin films with increasing Nb content

Diana Mardare, Abdullah Yildiz, Mihaela Girtan, Alina Manole, Marius Dobromir et al.

Citation: J. Appl. Phys. **112**, 073502 (2012); doi: 10.1063/1.4757007
View online: http://dx.doi.org/10.1063/1.4757007
View Table of Contents: http://jap.aip.org/resource/1/JAPIAU/v112/i7
Published by the American Institute of Physics.

Related Articles

Structure determination of thin CoFe films by anomalous x-ray diffraction
J. Appl. Phys. 112, 074903 (2012)

Multi-scale order in amorphous transparent oxide thin films
J. Appl. Phys. 112, 054907 (2012)

Growth of continuous and ultrathin platinum films on tungsten adhesion layers using atomic layer deposition techniques
Appl. Phys. Lett. 101, 111601 (2012)

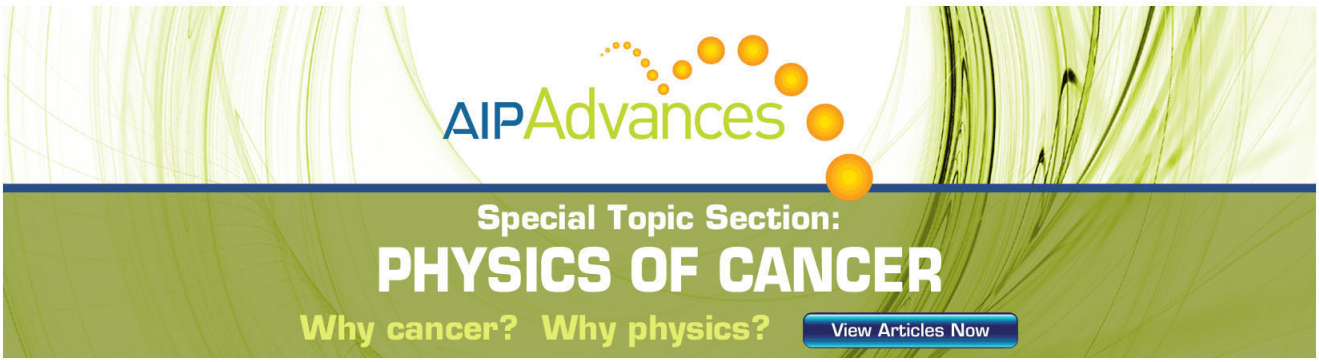
Effect of tip polarity on Kelvin probe force microscopy images of thin insulator CaF2 films on Si(111)
Appl. Phys. Lett. 101, 083119 (2012)

Epitaxial growth and metal-insulator transition of vanadium oxide thin films with controllable phases
Appl. Phys. Lett. 101, 071902 (2012)

Additional information on J. Appl. Phys.

Journal Homepage: http://jap.aip.org/
Journal Information: http://jap.aip.org/about/about_the_journal
Top downloads: http://jap.aip.org/features/most_downloaded
Information for Authors: http://jap.aip.org/authors

ADVERTISEMENT



Downloaded 02 Oct 2012 to 79.112.24.127. Redistribution subject to AIP license or copyright; see http://jap.aip.org/about/rights_and_permissions

Surface wettability of titania thin films with increasing Nb content

Diana Mardare,[1,a)] Abdullah Yildiz,[2] Mihaela Girtan,[3] Alina Manole,[1] Marius Dobromir,[1] Mihaela Irimia,[1] Catalin Adomnitei,[1] Nicoleta Cornei,[4] and Dumitru Luca[1]
[1]*Faculty of Physics, Alexandru Ioan Cuza University, 11 Carol I Blvd., 700506 Iasi, Romania*
[2]*Department of Energy Systems Engineering, Faculty of Engineering and Natural Sciences, Yıldırım Beyazıt University, 06030 Ankara, Turkey*
[3]*Photonics Laboratory, Angers University, 2, Bd. Lavoisier, 49045 Angers, France*
[4]*Faculty of Chemistry, Alexandru Ioan Cuza University, 11 Carol I Blvd., 700506 Iasi, Romania*

(Received 27 July 2012; accepted 30 August 2012; published online 1 October 2012)

TiO_2 and TiO_2/Nb amorphous thin films were grown on glass substrates by a sol-gel technique (spin coating). Films' surface composition, structure, and morphology were derived from x-ray photoelectron spectroscopy, x-ray diffraction, and atomic force microscopy data. The investigated films showed a smooth surface (roughness values below 5 nm). A separate surface wettability investigation showed that by increasing the Nb amount in pristine titania films results in a decrease of contact angle (CA) values from 40° to nearly 0°, thus, indicating a super-hydrophilic conversion under UV illumination. This conversion rate is greatly enhanced by increasing the Nb content, the surface super-hydrophilic behavior occurring after a couple of minutes in the TiO_2/Nb samples, but after 4 h in the pristine titania specimen. The current results are discussed in terms of the optical band gap shift towards higher energies, by increasing the Nb content in the films, a process explained based on small polaron hopping model. © *2012 American Institute of Physics*. [http://dx.doi.org/10.1063/1.4757007]

I. INTRODUCTION

Titanium dioxide (TiO_2) has been regarded as a material with attractive properties such as high oxidative power, large band gap, high dielectric constant, etc.[1–3] Since the discovery of the low resistivity (ρ) down to 2×10^{-4} Ω cm and high optical transmittance (95%) in epitaxial Nb-doped TiO_2 (NTO) films,[4–7] titanium oxide-based thin films have also attracted attention as a promising transparent conducting oxide (TCO) able to replace the more expensive films of indium tin oxide (ITO). The NTO materials can cover an important number of applications (optical film devices, capacitors in microelectronics, high-density dynamic-memory applications, gas sensors, transparent electrodes, etc.).[8–13]

There are many convenient methods to deposit TiO_2 thin films with adjustable properties: reactive sputtering, sol–gel, spray pyrolysis, etc.[1,2,8–13] Compared with other techniques, the sol–gel method offers important advantages, such as the possibility to deposit on complex-shaped substrates, easy control of the doping level, relatively inexpensive starting materials, and simple equipment. The objective of this paper is to quantitatively assess the effect of Nb concentrations on some physical properties of TiO_2 thin films.

II. EXPERIMENTAL

Uniform TiO_2 and TiO_2:Nb thin films have been deposited on glass substrates, using the sol-gel technique.[14] The solutions for the synthesis of the investigated films were prepared by dissolving titanium tetraisopropoxide $Ti(OC_4H_6)_4$ and niobium pentaethoxide $Nb(OC_2H_5)_5$ in absolute ethanol. First, 6 ml of ethanol were mixed with 0.5 ml titanium tetraisopropoxide and with 0.5 ml hydrochloric acid (used as stabilizer). The mixture was stirred for 10 h under N_2 atmosphere. Then, $Nb(OC_2H_5)_5$ was added in increasing quantities, the stirring was continued for 2 h. Solutions with different Nb contents were prepared, the atomic ratio $(Ti/Nb)_{sol.}$ being given in Table I. The corresponding films were deposited on glass substrates by spin coating with spinner angular speeds ranging between 2000 and 3000 rpm. The as-deposited films were first dried for 1 h at 100 °C, then annealed at 500 °C for 1 h. We denote the TiO_2 reference sample as S0, and S1, S2, S3—the NTO films with increasing niobium content.

The values of the films thickness, determined by ellipsometry, with a Horiba Jobin Yvon UVISEL VIP ellipsometer, are given in Table I. The structure of the films was investigated by x-ray diffraction (XRD), using a Bruker-AXS, D8 Advance diffractometer (CuK_α radiation, 40 mA, 40 kV), while their morphology was visualised by atomic force microscopy (AFM), using a Thermomicroscope Autoprobe LP Research, operated in contact mode. The elemental composition in the surface region was investigated by x-ray photoelectron spectroscopy (XPS). The spectra were recorded using a Physical Electronics PHI 5000 VersaProbe instrument, equipped with a mono-chromated Al K_α x-ray source (1486.6 eV). The photoelectrons were collected at a take-off angle of 45°. The sample surfaces (1×1 cm^2) were cleaned under ultra high vacuum (UHV) conditions, by sputtering with an Ar^+ ion beam (3 keV, 4 μA). The surface quantification was done following the standard procedure,[15] using the Ti 2*p*, O 1*s*, and Nb 3d XPS narrow spectra. Peak deconvolution has been done using the PHI-MULTIPAK software, and the elemental atomic concentration was calculated from the peak

a)Author to whom correspondence should be addressed. Electronic mail: dianam@uaic.ro.

 © 2012 American Institute of Physics

Downloaded 02 Oct 2012 to 79.112.24.127. Redistribution subject to AIP license or copyright; see http://jap.aip.org/about/rights_and_permissions

TABLE I. The thickness of the samples (d); the root mean square roughness (R_{rms}); the optical band gap (E_g); Ti/Nb atomic concentration ratio in the starting solutions; Ti/Nb atomic concentration ratio as resulted from XPS; the elemental composition from the XPS data.

Sample	d (nm)	R_{rms} (nm)	E_g (eV)	$(Ti/Nb)_{sol.}$	$(Ti/Nb)_{XPS}$	Elemental composition from XPS				
S0	99	2.1	3.25	0.0	0.0	O (at. %)	Ti (at. %)	Nb (at. %)	x	δ
S1	78	2.6	3.41	8.18	11.39	67.8	29.6	2.6	0.08	2.10
S2	86	2.9	3.53	1.02	1.45	68.1	18.9	13.0	0.40	2.13
S3	97	4.8	3.58	0.50	0.46	69.4	9.6	21.0	0.69	2.27

surface areas, taking into account the sensitivity factors of the analyzed elements.[16]

The CA measurements have been performed with a Data Physics OCA 15EC goniometer, at room temperature and 75% relative humidity, in a sessile drop arrangement. The final values were obtained by averaging five CA values mesured at different locations on the films surface. Water drop volumes as low as 0.5 μl have been used to avoid gravitational drop shape alteration and to diminish evaporation effects during CA measurements. For the hydrophilic conversion process, films surfaces were irradiated with a high-pressure Hg lamp (1 mW/cm^2) with emission lines in both UV and visible ranges.

The optical transmittance and reflectance spectra were recorded at room temperature, in the 300–1000 nm wavelength range with non-polarized light, using a double beam Perkin–Elmer Lambda 19 UV-Vis spectro-photometer.

III. RESULTS AND DISCUSSION

The elemental composition of the investigated films, as derived from the XPS investigation is given in Table I. The O 1s spectra are almost the same for all the samples. A representative O 1s XPS spectrum is given in Fig. 1(a). The spectra were deconvoluted into a main component at 529.2 eV, corresponding to lattice oxygen and a secondary one at 530.4 eV, due to hydroxyl groups. For the samples with higher Nb content (S_2 and S_3), a slight shift (approx. 0.4 eV) towards higher binding energies can be observed for the second peak. The area ratio of the two components is the same for the TiO_2/Nb samples (A1/A2 is equal to 80/20).

The Ti 2p XPS spectra of all the TiO_2/Nb samples demonstrate the presence of both Ti^{4+} and Ti^{3+} states (Fig. 1(b)). The binding energies corresponding to the Ti^{4+} $2p_{3/2}$ and $2p_{1/2}$ are 457.8 ± 0.2 eV and 463.4 ± 0.2 eV, respectively. For the reduced state, the binding energy, corresponding to the Ti^{3+} $2p_{3/2}$, is 455.9 ± 0.2 eV, and the one corresponding to the Ti^{3+} $2p_{1/2}$ is 461.5 ± 0.2 eV. The titanium concentration decreases with the increase of the Nb content in the samples.

The Nb 3d XPS spectra feature three well-resolved peaks: one around 204.0 eV corresponding to the Nb^{4+} state, the second one at about 206.2 eV, corresponding to the Nb $3d_{5/2}$, and the third one, around 208.8 eV, corresponding to the Nb $3d_{3/2}$ state[17] (Fig. 2).

By comparing the two Ti/Nb atomic concentration ratios—the ones expected from the starting solutions for film synthesis, and the results from the XPS data, one can observe that the films retained a slightly different amount of Nb, compared with the amounts introduced in the synthesis report (see Table I). From the XPS data, one can derive the values of x and δ in the formula $Ti_{1-x}Nb_xO_\delta$. While x varied between 0.08 and 0.69, δ varied between 2.10 and 2.27, showing that the samples are slightly overoxidized (Table I).

The structural analysis performed by XRD shows amorphous structures for the investigated samples.[14] This can be due to the low film thickness, causing the XRD patterns of the film to be covered by large effect of amorphous glass substrate.

The AFM studies revealed very smooth surfaces for all the studied films, featuring root mean square roughness (R_{rms}) values below 5 nm (Table I). R_{rms} increases with the increase of the Nb content, almost doubling its value for sample S3 (Fig. 3).

Two mechanisms are responsible for the decreasing of the light intensity upon passing through the films, namely

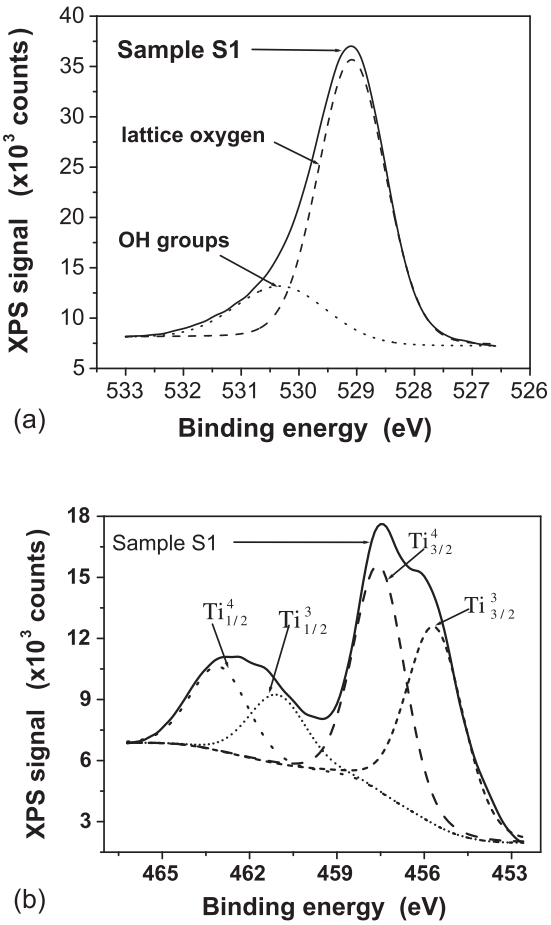


FIG. 1. A typical O 1s XPS spectrum (a) and Ti 2p XPS spectrum (b).

Downloaded 02 Oct 2012 to 79.112.24.127. Redistribution subject to AIP license or copyright; see http://jap.aip.org/about/rights_and_permissions

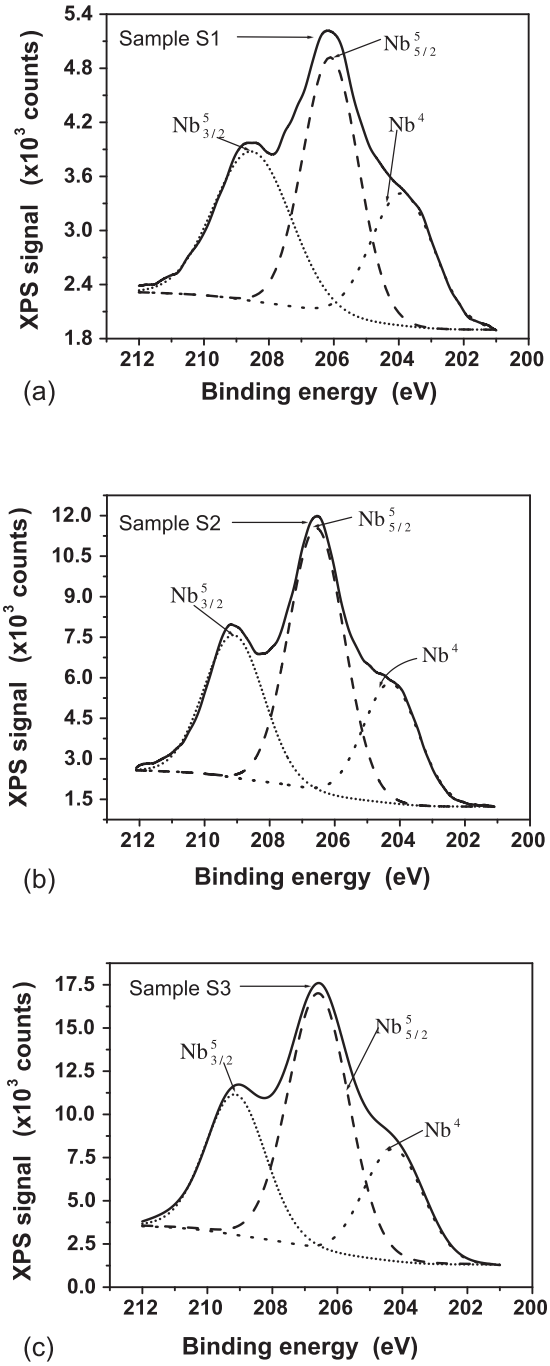


FIG. 2. Nb 3d XPS spectra of the investigated samples.

absorption and scattering. It is well known that the titanium oxide thin films are transparent in the visible range, and absorbent in ultraviolet, their absorption edge being situated in the near UV range, having values depending on their phase content.[18,19]

The absorption coefficient, α, can be obtained from the following relation:[20]

$$T = [(1-R)^2 \exp(-\alpha d)]/[1 - R^2 \exp(-2\alpha d)], \quad (1)$$

where T and R are the optical transmittance and optical reflectance at a certain wavelength, d is the thickness of the film. For wavelengths values, where the scattering loss are

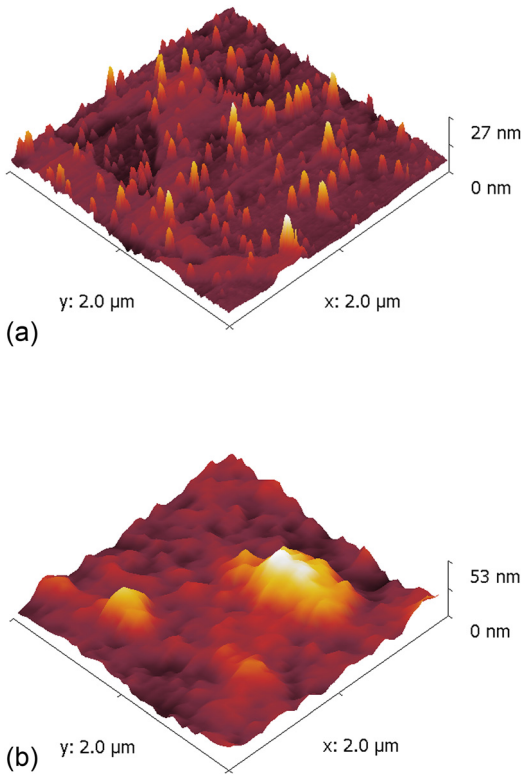


FIG. 3. 3-D AFM images of: (a) sample S0 (pristine TiO_2); (b) sample S3 (with the highest Nb content).

dominated by the fundamental absorption of light, we could neglect the term containing R^2, therefore, much simpler relation can be used to determine the absorption coefficient

$$\alpha = d^{-1} \ln[(1-R)^2/T]. \quad (2)$$

In the vicinity of the fundamental absorption, we may consider that the indirect allowed transition dominates over the optical absorption, according to the relation:[18,19]

$$(\alpha h\nu)^{1/2} = A_i(h\nu - E_g), \quad (3)$$

where $h\nu$ is the photon energy, A_i is a characteristic parameter independent of photon energy for respective transitions, and E_g is the optical band gap. The values of E_g obtained by extrapolating the linear part of $(\alpha h\nu)^{1/2} = f(h\nu)$ dependence to $(\alpha h\nu)^{1/2} = 0$ are listed in Table I. The correlation coefficients of the linear fits varied from 0.998 for sample S0 to 0.996 for Sample S3.

The values of E_g are much higher than those reported in the literature (3.11 eV for the rutile phase[21] and 3.2 eV for the anatase phase[22]), or than those previously obtained in our former studies.[18,19] An explanation might be related to the size quantum effects, the thickness of the films under study being lower than 100 nm, while in Refs. 18 and 19, we dealt with thicker films (>250 nm). From Fig. 4 and Table I, a shift of the optical band gap values towards higher energies can be observed. While this observation accords well with some other references,[23,24] it is not sustained by other researches.[25] That is why we have tried to explain this increase of the optical band gap, with the increase of the Nb content. The

Downloaded 02 Oct 2012 to 79.112.24.127. Redistribution subject to AIP license or copyright; see http://jap.aip.org/about/rights_and_permissions

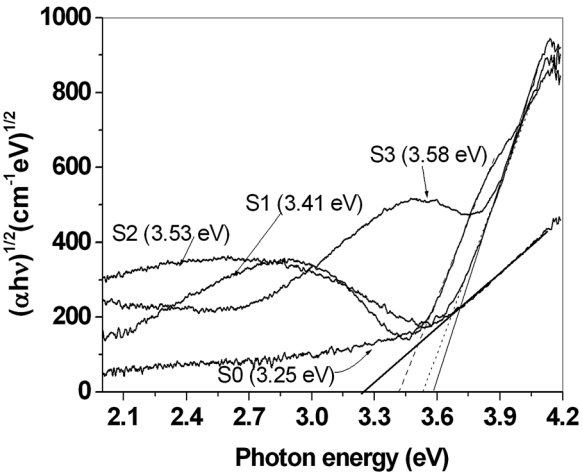


FIG. 4. The $(\alpha h\nu)^{1/2}$ vs. $h\nu$ plots.

explanation is made from a polaronic point of view, being based on our previous results.[14] In Ref. 14, we have dealt with the electrical properties of similar films and established that the temperature-dependent conductivity of the films is dominated by the phonon-assisted small polaron hopping (SPH) in non-adiabatic regime. The room temperature electrical resistivity of the titanium oxide films decreases gradually by increasing the Nb concentration, which confirms that Nb impurities act as donors, resulting in an *n*-type extrinsic semiconducting behavior for TiO_2/Nb thin films.[7,14,26,27] The lowest room temperature electrical resistivity value of our films is obtained for the highest Nb concentration (225 Ω cm), while in the absence of the Nb atoms, resistivity values as high as 152×10^5 Ω cm can be noticed.

From the polaronic viewpoint, the Nb percentage-dependent shift of the values of the optical band gap towards higher energies may be explained as follows: First of all, the electronic excitations for TiO_2, which is an ionic crystal, should be different from common semiconductors. In contrast, in an ionic crystal, the electron excitation spectrum can be described by the SPH model. In this case, the thermally excited polarons locate at the small polaron band, which is lower than the conduction band edge.[28] These materials exhibit the formation of small polarons, and the electrical conduction occurs by hopping of small polarons between the ions of low and high valence states. In our case, the increase of the electrical conductivity by increasing the Nb content may be related to the filling of valence states resulting in the increase of hopping rate. The distance that the electron crosses by tunneling in one hopping event decreases upon increasing the donor (Nb) concentration. Subsequently, the excited states of the localized electrons (originally trapped on Ti^{4+} sites) begin to overlap with the empty states on the neighboring Ti^{3+} sites and, as a result, the polaron band becomes more extended. This new polaronic situation might lead to a widening in the band gap.

Although governed by different mechanisms, the photocatalytic and hydrophilic properties of the TiO_2 materials are closely correlated, acting in the same direction. For this reason, CA measurements can be routinely used to indirectly assess the photocatalytic efficiency of the TiO_2 films. The hydrophilic properties are ascribed to the reducing effect of photoelectrons on Ti^{4+} to Ti^{3+}. The expulsion of oxygen anions from the Ti^{3+} sites and the occurrence of oxygen vacancies favor the occurrence of hydroxyl groups, responsible for surface hydrophilicity.[2] For CA smaller than 10°, the surface is considered super-hydrophilic.[1,2]

As seen from Fig. 5, the TiO_2/Nb thin films feature initial contact angles lower than 5°, thus, their surface is highly super-hydrophilic, under normal conditions (even without UV irradiation). To analyze the photo-induced hydrophilic conversion processes at the samples surface, the contact angle (θ) was monitored as a function of the irradiation time. After only 10 min under UV illumination, all the TiO_2/Nb thin films reaches CA values close to 0°, while the pristine titania sample (with an initial CA around 40°) needs about 4 h of UV illumination to reach contact angle values smaller than 10°.

The small crystallite size in the titania films is related with to higher photocatalytic efficiency and the hydrophilic activity of TiO_2 surface.[29] In our case, all the films are very thin, making the detection of small crystallite very difficult. This might explain the super-hydrophilic properties of the TiO_2/Nb films,[29] but cannot be claimed to support the behavior of the pristine samples.

A more reasonable explanation could be related to the band gap values (E_g) of the studied samples, since it has been demonstrated that the lifetime values of the electron-hole pairs occurring upon UV irradiation in the surface region are directly proportional to E_g.[30] XPS studies revealed the presence of the Ti^{3+} states in the pristine titania and TiO_2/Nb samples. It had to be mentioned that the samples under study were sputtered with argon ions before XPS investigation, to remove the contamination layer. As previously reported,[31,32] Ti^{3+} states can occur during this operation. But even so, one can observe from Fig. 6 that Ti^{3+} $2p_{3/2}$ peak area increases with the Nb content.

Since the hydrophilic properties are ascribed to the presence of these Ti^{3+} states, the above-mentioned observation,

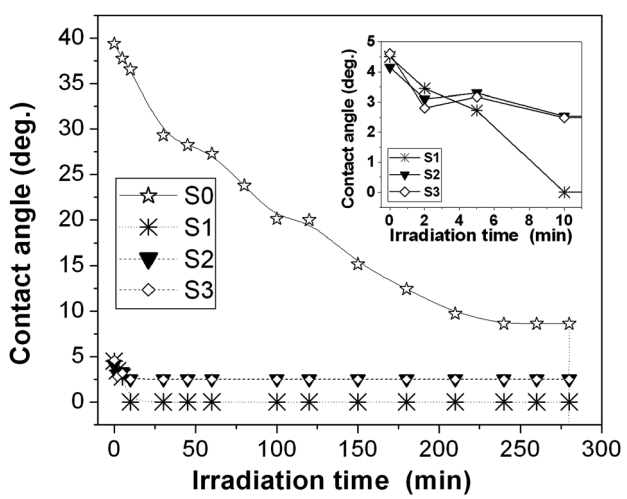


FIG. 5. Contact angle vs. UV irradiation time plots for the pristine TiO_2 and TiO_2/Nb samples. The inset shows the same dependences for a TiO_2/Nb sample, when the super-hydrophilicity state is achieved.

Downloaded 02 Oct 2012 to 79.112.24.127. Redistribution subject to AIP license or copyright; see http://jap.aip.org/about/rights_and_permissions

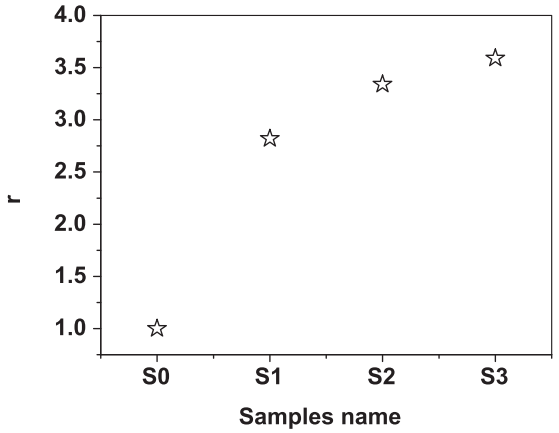


FIG. 6. The ratio (r) between the areas of Ti^{3+} $2p_{3/2}$ peaks for the TiO_2/Nb samples and the corresponding area of the peak for the pristine TiO_2 film (obtained from XPS spectra).

certainly help us to better understand the change in the hydrophilic properties of titania films by increasing the Nb content.

IV. CONCLUSIONS

Amorphous smooth $Ti_{1-x}Nb_xO_\delta$ films (with $0.08 < x < 0.69$ and $2.10 < \delta < 2.27$) have been fabricated by the sol-gel technique (spin coating). The presence of Nb in TiO_2 films determines the samples Nb/TiO_2 to be highly super-hydrophilic, with initial CA values lower than 5°, while TiO_2 sample presents an initial CA around 40°. Comparing the 4 h time of UV illumination, needed by the pristine film to reach CA of 8.8°, and the 10 min n eeded in the case of the TiO_2/Nb films to reach CA values around 0°, one can easily see the superiority of the TiO_2/Nb samples as concern the hydrophilic properties. The optical band gap was found to increase by increasing the Nb content in the films, the explanation being based on the SPH model.

ACKNOWLEDGMENTS

This work was supported by CNCSIS Contract No. PCCE-ID_76/2010. Marius Dobromir and Mihaela Irimia acknowledge the financial support from the Romanian POS-DRU/89/1.5/S/49944 and POS-DRU/88/1.5/S/47646 research programs, respectively.

[1]A. Fujishima, X. Zhang, and D. A. Tryk, Surf. Sci. Rep. **63**, 515 (2008).
[2]A. Fujishima, T. N. Rao, and D. A. Tryk, J. Photochem. Photobiol. C **1**, 1 (2000).
[3]M. Stamate, Thin Solid Films **372**, 246 (2000).
[4]Y. Furubayashi, T. Hitosugi, Y. Yamamoto, K. Inaba, G. Kinoda, Y. Hirose, T. Shimada, and T. Hasegawa, Appl. Phys. Lett. **86**, 252101 (2005).
[5]T. Hitosugi, A. Ueda, S. Nakao, N. Yamada, Y. Furubayashi, Y. Hirose, S. Konuma, T. Shimada, and T. Hasegawa, Thin Solid Films **516**, 5750 (2008).
[6]Y. Furubayashi, T. Hitosugi, Y. Yamamoto, Y. Hirose, G. Kinoda, K. Inaba, T. Shimada, and T. Hasegawa, Thin Solid Films **496**, 157 (2006).
[7]T. Hitosugi, Y. Furubayashi, A. Ueda, K. Itabashi, K. Inaba, Y. Hirose, G. Kinoda, Y. Yamamoto, T. Shimada, and T. Hasegawa, Jpn. J. Appl. Phys., Part 2 **44**, L1063 (2005).
[8]M. Epifani, A. Helwig, J. Arbiol, R. Diaz, L. Francioso, P. Siciliano, G. Mueller, and J. R. Morante, Sens. Actuators, B **130**(2), 599 (2008).
[9]Y. Sawada and Y. Taga, Thin Solid Films **116**, L55 (1984).
[10]A. M. More, J. L. Gunjakar, and C. D. Lokhande, Sens. Actuators, B **129**(2), 671 (2008).
[11]D. Mardare, N. Iftimie, and D. Luca, J. Non-Cryst. Solids **354**, 4396 (2008).
[12]N. Iftimie, D. Luca, F. Iacomi, M. Girtan, and D. Mardare, J. Vac. Sci. Technol. B **27**(1), 538 (2009).
[13]M. Crisan, A. Braileanu, M. Raileanu, D. Crisan, V. S. Teodorescu, R. Birjega, V. E. Marinescu, J. Madarász, and G. Pokol, J. Therm. Anal. Calorim. **88**, 171 (2007).
[14]A. Yildiz and D. Mardare, Philos. Mag. **91**(34), 4401 (2011).
[15]J. F. Watts and J. Wolstenholme, *An Introduction to Surface Analysis by XPS and AES* (John Wiley & Sons, Chichester, 2003).
[16]J. F. Moulder, W. F. Stickle, P. E. Sobol, and K. D. Bomben, *Handbook of X-Ray Photolectron Spectrosopy* (ULVAC-PHI Japan, Physical Electronics, USA, 1995).
[17]Y. Liu, J. M. Szeifert, J. M. Feckl, B. Mandlmeier, J. Rathousky, O. Hayden, D. Fattakhova-Rohlfing, and T. Bein, ACS Nano **4**(9), 5373 (2010).
[18]D. Mardare and G. I. Rusu, J. Non-Cryst. Solids **356**, 1395 (2010).
[19]D. Mardare and G. I. Rusu, Mater. Lett. **56**, 210 (2002).
[20]T. S. Moss, *Optical Properties of Semiconductors* (Butterworths, London, 1959).
[21]N. Daude N. C. Gout, and C. Jouanin, Phys. Rev. B **15**, 3229 (1977).
[22]H. Tang, K. Prasad, R. Sanjinès, P. E. Schmid, and F. Lévy, J. Appl. Phys. **75**, 2042 (1994).
[23]Y. Sato, H. Akizuki, T. Kamiyama, and Y. Shigesato, Thin Solid Films **516**, 5758 (2008).
[24]K.-H. Hung, P.-W. Lee, W.-C. Hsu, H. C. Hsing, H.-T. Chang, and M.-S. Wong, J. Alloys Compd. **509**, 10190 (2011).
[25]A. Mattsson, M. Leideborg, K. Larsson, G. Westin, and L. Österlund, J. Phys. Chem. B **110**, 1210 (2006).
[26]D. Mardare and G. I. Rusu, Mater. Sci. Eng., B **75**, 68 (2000).
[27]A. Yildiz, S. B. Lisesivdin, M. Kasap, and D. Mardare, Physica B **404**, 1423 (2009).
[28]G.-L. Li, W.-X. Li, and C. Li, Phys. Rev. B **82**, 235109 (2010).
[29]T. M. Wang, S. K. Zheng, W. C. Hao, and C. Wang, Surf. Coat. Technol. **155**, 141 (2002).
[30]W. C. Hao, S. K. Zheng, C. Wang, and T. M. Wang, J. Mater. Sci. Lett. **21**(20), 1627 (2002).
[31]S. Hashimoto, A. Tanaka, A. Murata, and T. Sakurada, Surf. Sci. **556**, 22 (2004).
[32]A. Manole, V. Dăscăleanu, M. Dobromir, and D. Luca, Surf. Interface Anal. **42**, 947 (2010).

Downloaded 02 Oct 2012 to 79.112.24.127. Redistribution subject to AIP license or copyright; see http://jap.aip.org/about/rights_and_permissions